Proceedings of the Canadian Society for Mechanical Engineering International Congress 2022
CSME Congress 2022
June 5-8, 2022, Edmonton, AB, Canada

CFD SIMULATION OF CONDENSATION HEAT TRANSFER IN MINI/MICRO-CHANNELS—APPLICATION IN WASTE HEAT RECOVERY

Ehsan Ebrahimnia-Bajestan[1], Mehrdad Gharibnavaz[2*], Mingchao Jin [1], Ri Li[1*], Joshua Brinkerhoff[1], Abbas Milani[1]
[1]School of engineering, University of British Columbia, Kelowna, BC, Canada
[2]FEED Engineering Inc., Vancouver, BC, Canada
* mgharib@feedengineering.com; sunny.li@ubc.ca

Abstract— The recovery of waste heat from low-temperature flue gas can be improved by capturing the latent heat part through the condensation of the vapor component. For this purpose, investigating the important parameters in designing efficient heat exchangers is necessary. Therefore, this study aims to develop a reliable model for simulating condensation heat transfer to help understand the involved phenomena and optimize the low-temperature waste heat recovery systems. The studied flue gas was a mixture of multicomponent non-condensable gas and water vapor released by electric generators or furnaces. In this study, mini-channel heat exchangers were explored in order to maximize heat transfer surface area and minimize heat exchanger size. A CFD model in Ansys Fluent was developed to analyze the condensation heat transfer in a mini-channel. Model accuracy was confirmed by comparison with experimental data available in the literature. Using the model, we then investigated the temperature field, vapor concentration, heat flux, and film thickness along the channel at inlet velocities ranging from 0.5 to 10 m/s (i.e., the corresponding Reynolds numbers of 31 to 617). The model has been found to be a powerful tool for predicting condensation heat transfer in the flue gas and designing heat exchangers for latent heat recovery.

Condensation heat transfer; CFD; waste heat recovery; non-condensable gas; mini-channel

I. INTRODUCTION

A significant amount of energy (almost 60%) is wasted through heat loss in power generators, including natural gas ones. Waste heat is a by-product of many industrial processes and is continually produced around the globe in enormous amounts. Recovering the waste heat can significantly increase the efficiency of the energy systems and reduce the use of fossil fuel.

A heat recovery unit, which is primarily a heat exchanger, transfers heat from the flue gas to a cooling fluid, such as water. One challenge in recovering heat from low-temperature flue gas is the low sensible heat due to the low temperature difference between gas and coolant. The solution is to recover both sensible and latent heat from flue gas, which contains vapor water. Additionally, the use of micro- or mini-channels can increase the surface area for this heat transfer.

When the temperature of channel wall is lower than the dew point of flue gas, vapor transfers from the mixture and condenses on the wall. This results in a mass transfer boundary layer near the condenser wall, and in the boundary layer the concentration of non-condensable gas (NCG) is higher than the bulk flow. This boundary layer creates resistance to the transfer of vapor and in turn to the condensation. As compared to the condensation of pure vapor, the presence of even a small amount of non-condensable gas in the mixture can dramatically affect condensation rate [1]. Therefore, the condensation mechanism of vapor-NCG mixture is a complex phenomenon involving multiphase flow, heat and mass transfer, where detailed understanding of the mechanism is essential for designing the heat exchanger. CFD simulation is considered as a powerful approach for further analysis of the condensation process in different geometries [2].

A common approach for simulating NCG-vapor mixture condensation is based on modeling a condensation mass flux, which is then incorporated as source terms into the governing equations for the cells adjacent to the condensing interface. These models that work based on vapor concentration gradient near the wall are referred as diffusion-based models.

Zschaeck et al. [3] and Punetha and Khandekar [4] simulated the condensation of vapor in the presence of NCGs flowing through the tubes and channels, considering a mass source (sink) at the condensing wall and neglecting the condensate film thickness on the wall. They employed the Wall Condensation Model in ANSYS CFX for these simulations. Similarly, Kumar et al. [5] developed a CFD model on OpenFOAM to predict vapor condensation on walls in the presence of NCGs focusing on large scale applications. They compared the computational cost of the simulations when the condensation mass flux is considered as i) a mass flux boundary condition at the wall, and ii) source terms in the cells adjacent to the wall.

Few CFD studies have modeled the condensing film thickness along with the heat and mass transfer in the mixture

flow. Li [6] using Fluent CFD code, developed a model for wall condensation of vapor-gas mixture of medium to high concentrations of non-condensable gas in a vertical tube. The condensation-related source terms were accounted for near the wall. For the mass conservation, the source term is the amount of water vapor condensed on the wall. Condensed mass was modeled using the mass concentration gradient at the interface between the gas mixture and the condensate film. Multiplying the mass source term by local mixture velocity at the interface yielded the source term for the momentum equation. Similarly, for the energy equation the mass source term should be multiplied by vapor enthalpy at the interface. They also solved the film thickness through the Nusselt approximation. This method proposes an analytical solution for velocity and temperature of condensate film, through simplifying the governing equations by neglecting the interfacial shear and momentum effects. Recently, Liu et al. [7] simulated condensation heat transfer in the tube bundle channels under natural convection condition. They predict the flow and thickness of the liquid film on the wall using the Eulerian wall film (EWF) model available in ANSYS Fluent.

In the present study, the condensation heat transfer of water vapor in the presence of high concentration of multicomponent non-condensable gas has been simulated for application in waste heat recovery. The Eulerian Wall Film model in ANSYS Fluent was used to predict the condensing film formed on the walls during condensation, by solving a set of mass, momentum, and energy conservation equations. Mini-channel heat exchangers are desirable for the studied application because of the relatively large heat transfer surface area. In this paper, condensation heat transfer of flue gas in a mini-channel has been numerically analyzed. To the best of our knowledge this is the first time that this problem with this condensation model is examined.

II. METHODLOGY

A. Physical model

In this research, the flow, heat, and mass transfer of the flue gas in a mini-channel has been investigated. Table I lists the components of the studied gas mixture and their concentrations. The Table also includes the properties of the components at the average temperature of the inlet flow and the wall. Only the heat capacity values of the gasses are temperature dependent using ANSYS Fluent database.

TABLE I. FLUE GAS COMPONENTS

Components	H_2O	N_2	CO_2	O_2
Mole fraction (%)	18	71	10	1
Density (kg/s)	0.11	1.22	1.79	1.30
Thermal conductivity (W/m K)	0.022	0.028	0.014	0.025
Viscosity (Pa s)	1.03×10^{-5}	1.97×10^{-5}	1.37×10^{-5}	1.92×10^{-5}
Molecular weight (g/mol)	18.01	28.01	44.01	31.99

For the liquid water, the density, viscosity, thermal conductivity, and specific heat capacity were employed at the wall temperature, as 998 kg/m^3, 9.59×10^{-4} Pa s, 0.606 W/mk, 4181 J/kgK, respectively, with the condensation latent heat of 2449 kJ/kg.

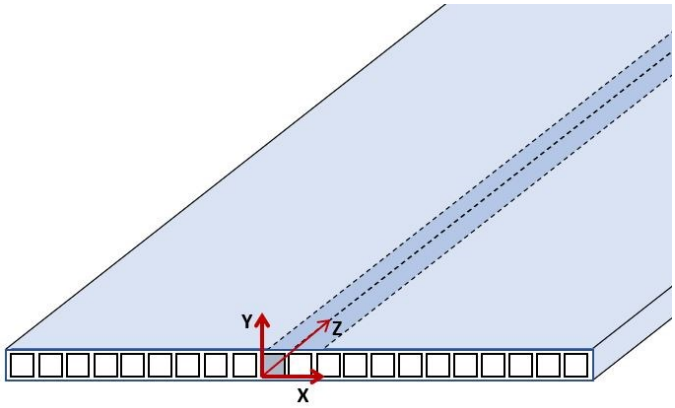

Figure 1 The schematics of studied mini-channel

Taking into account multiport micro-heat exchangers available in the market, one of the mini-channels, as shown in Fig. 1, with a square cross-section of 1×1 mm^2 and a length of 100 mm was selected to study the condensation model. Liquid water as the coolant passes over the channel and flue gas flows inside the channel. In this study, the wall thickness was not modeled and the wall temperature was assumed constant for all walls because of the relatively high thermal conductivity of the metal wall. However, we are studying a channel with a finite wall thickness and will report as a paper in the future.

B. Numerical model

The following assumptions are used to model condensation heat transfer in flue gas.

a. The vapor-NCG mixture is an incompressible ideal gas,

b. Only filmwise condensation occurs; dropwise condensation was not considered,

c. The mixture and liquid flows are laminar,

d. The system is in a steady state,

e. The velocity, temperature, and gas concentration profiles are uniform at the inlet,

f. Gravity and surface tension forces are negligible.

Accordingly, the governing equations are as follows,

Mass conversion:

$$\nabla\cdot(\rho\vec{v}) = S_m \quad (1)$$

Momentum conservation:

$$\nabla\cdot(\rho\vec{v}\vec{v}) = -\nabla p + \nabla\cdot\tau + \rho\vec{g} + S_v \quad (2)$$

Energy conservation:

$$\nabla\cdot[(\rho E + p)]\vec{v} = \nabla\cdot(k\,\nabla T - \sum_j h_j \vec{J}_j) + S_h \quad (3)$$

In the above equations, $\vec{v}$, p, T, E, and τ are velocity, pressure, temperature, and internal energy, and shear stress for the mixture, respectively. Density, ρ, and thermal conductivity, k, are mixture's properties. J_j is the diffusion flux of jth component—four components in this study—due to the concentration gradient, and h_j is sensible enthalpy of jth component.

The local mixture's properties were computed based on the local mass fraction average of the pure species properties as,

$$\varphi = \sum_{i=1}^{4} \varphi_i Y_i \quad (4)$$

where φ can be thermal conductivity, viscosity, and specific heat capacity, reported in Table I for each component.

Using the ideal gas law for an incompressible flow, the solver computed the density as,

$$\rho = \frac{p_{op}}{RT\ \sum_{i=1}^{4} Y_i/M_{w,i}} \quad (5)$$

where, P_{op} = 101.325 kPa, and R = 8.314 J/mole, are the operating temperature, and the universal gas constant. $M_{w,i}$ denotes the molecular weight of component i available in Table I.

For local mass fraction of each component, Y_i, the convection-diffusion equation for component i in the mixture was solved using species transport model in ANSYS Fluent, given as [8],

$$\nabla\cdot(\rho\vec{v}\ Y_i) = -\nabla\cdot\vec{J}_i \quad (6)$$

Eq (4) was solved for three components of the flue gas (see Table I). Then, the local concentration of the 4th species with the overall largest fraction, which is nitrogen, was computed based on the fact that the total mass fraction of the mixture is equal to one.

In the absence of Soret effect, the diffusion flux of species i, which arises due to concentration gradients can be written using Fick's law for the laminar flow, as follows.

$$\vec{J}_i = -\rho\, D_{i,m}\ \nabla Y_i \quad (7)$$

Where $D_{i,m}$ donates the mass diffusion coefficient of component i in the mixture. This value was considered constant and equals to 2.88 ×10^{-5} m^2/s.

To model film-wise vapor condensation, the Eulerian Wall Film (EWF) model was applied, which predicts the liquid film thickness, velocity and temperature, by solving a set of mass, momentum, and energy conservation equations, defined as,

$$\frac{\partial \rho_l h}{\partial \mathrm{t}} + \nabla_s\cdot(\rho_l h\vec{v}_l) = \dot{m}''_v \quad (8)$$

$$\frac{\partial \rho_l h\vec{v}_l}{\partial \mathrm{t}} + \nabla_s\cdot\left(\rho_l h\vec{v}_l\vec{v}_l + \vec{D}_v\right) = -h\,\nabla_s P_{mixture} + \frac{3}{2}\tau_{fs} - 3\frac{\mu_l}{h}\vec{v}_l \quad (9)$$

$$\frac{\partial \rho_l hT_f}{\partial \mathrm{t}} + \nabla_s\cdot\left(\rho_l h\vec{v}_l T_f + \vec{D}_T\right) = \frac{1}{C_{p,l}}\left[\frac{2\,k_f}{h}\,(T_s + T_w - 2T_m) + \dot{m}''_v\, h_{fg}\right] \quad (10)$$

In these equations, h represents the film thickness. The subscripts of l, v, s, w, m donate liquid water, vapor, film surface, condenser wall, and film bulk. ∇_s stands for the surface gradient operator. D_v and D_T denote the differential advection terms.

On the right-hand side of film momentum conservation equation, the first term considers mixture flow pressure effects, the second and third terms includes shear forces on the gas-film and film-wall interfaces. On the right-hand side of energy equation, the first term represents the net heat flux on the gas-film and film-wall interfaces. The second term is the energy transfer due to the condensation. h_{fg} is the condensation latent heat equal to 2449 kJ/kg.

The condensation phase change rate of water vapor on the gas–film interface was modeled using the wall boundary layer model, defined as

$$\dot{m}''_v = \frac{-\rho\, D_{m,v}\,\partial Y_v/\partial n}{1 - Y_v} \quad (7)$$

This computed mass flux, with the unit of kg/m^2 s, is applied to the source terms of conservation equations for both gas mixture and liquid film. The subscript v donates vapor component in the mixture. The mass diffusion coefficient of vapor is $D_{m,v}$ =2.88 ×10^{-5} m^2/s.

The EWF model was coupled with the species transport model in ANSYS Fluent and activated on the wall defined as condenser to simulate the heat and mass transfer between water vapor in the mixture and the liquid water on the walls. This condensation model is triggered when the partial pressure of vapor in the gas mixture exceeds the vapor pressure at the film surface.

C. *Boundary conditions*

In this study, at the inlet of the channel, the mole fraction of each component was defined as listed in Table I, the temperature was 120 °C, and velocity (Reynolds number) ranged from 0.5 m/s (31) to 10 m/s (617). Boundary conditions applied to the channel walls were constant temperature of 20 °C, no slip, and no species diffusive flux. The outlet boundary condition was considered as pressure outlet.

D. *Solution methodology*

The governing equations were solved by ANSYS Fluent, discretized using the finite volume method. The coupled algorithm was used as the pressure-velocity coupling scheme. The convergence condition was achieved when the residuals are less than 10^{-7}.

A mesh study was carried out to analyze the mesh sensitivity of temperature, velocity, vapor fraction and liquid film thickness. Considering computational cost and accuracy, the cell numbers of 20×20 in the cross-section and 500 cells at the flow direction were chosen. Meshes are refined near the walls and the inlet.

E. *Validation study*

In order to validate the condensation model used in this study, two important parameters of wall heat flux and condensate film flow rate were compared with the experimental data of Ambrosini et al. [9]. These researchers conducted a benchmark study of filmwise condensation at the CONAN test facility for a vapor-air mixture flowing through a 0.32×0.32×2 m^3 channel. Considering the flow condition in the test channel, and confirmed by other researchers [4,10,11], 2D simulation is adequate for modeling this experimental study. For this validation study, we simulated a 3D symmetric model which is reflected the 2D model (similar to the geometry consideration in Ref. [4]).

Fig. 2 and Table II show the results of the comparisons. The legend is based on the name given to the test data. T30, V15, and V35 denote the test conditions, as nominal condenser wall temperature of 30°C, nominal inlet mixture velocity of 1.5 m/s, and 3.5 m/s, respectively. The mass fraction of vapor in the mixture for the cases of P10-T30-V15, and P10-T30-V35, are 0.41 and 0.27, respectively.

The predicted film flow rate shows a deviation of 3% compared to experimental data. The discrepancies of local surface heat flux from the experimental data are lower than 20%, except at Z= 1.64m and at the inlet. The high deviation of CFD simulations from CONAN experimental results at the entrance has been observed by other researchers [4,10,11]. The possible reasons can be the effects due to 3D symmetric modeling, nonuniformity of the inlet mixture velocity in the real case, and the entrance effects such as velocity overshoot in the simulation.

TABLE II. COMPARISON OF EXPERIMENTAL DATA [9] AND PRESENT NUMERICAL RESULTS FOR CONDENSATE FILM FLOW RATE

Case	P10-T30-V15		P10-T30-V35	
	Experimental	Numerical	Experimental	Numerical
Film flow rate (g/s)	2.28	2.28	2.97	3.06

In conclusion, these good agreements between experimental and numerical results demonstrates the ability of the present numerical approach for simulating filmwise condensation of vapor-NCG mixtures flows.

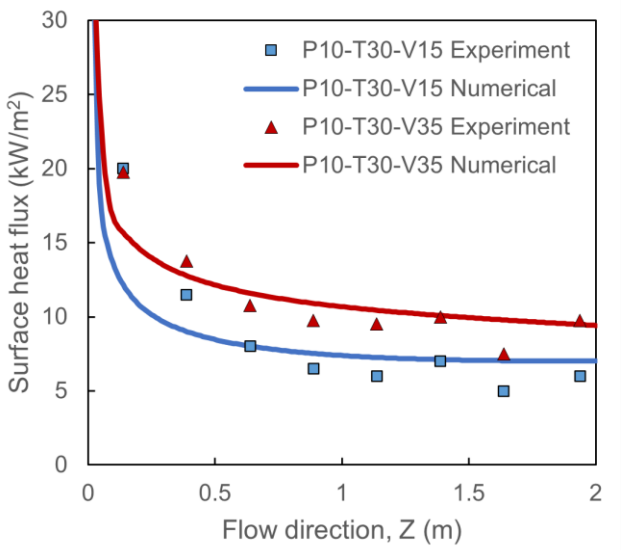

Figure 2 Variation of surface heat flux along the channel predicted by present numerical model compared to available experimental data of Ambrosini et al. (2009)

III. RESULTS AND DISCUSSION

This section discusses the condensation heat transfer simulation results in the mini-channel. As flue gas with a high concentration of NCG passes into the channel, water vapor begins to condense on the walls that have temperature below the saturation temperature of vapor. This results in formation of films of liquid water on the walls.

The vapor transfer to the liquid film is driven by the gradient of the vapor concentration in the mass transfer boundary layer, where the concentration of NCG is higher than the bulk flow. Fig. 3 shows the profile of vapor concentration at different cross sections, illustrating the lower concentration of vapor close to the wall.

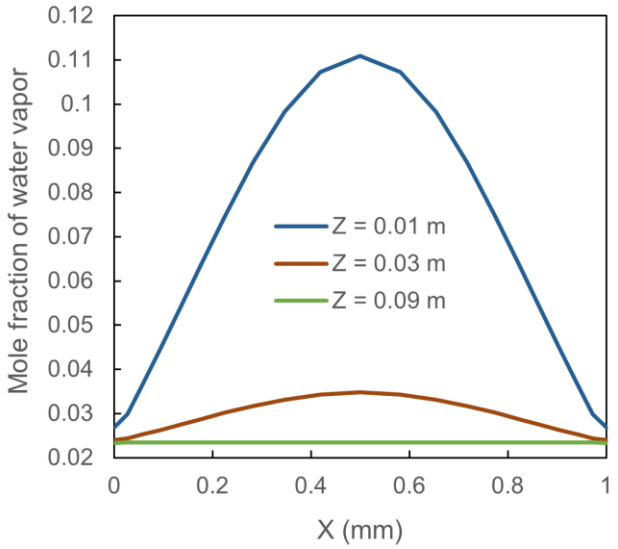

Figure 3 Variation of mole fraction of vapor normal to the channel wall for different cross sections at Y=0.5 mm; V_{in}= 5 m/s

The NCG layer acts as a barrier to condensation. Therefore, for an efficient waste heat recovery, it is necessary to have an adequately long channel to capture the majority of latent heat from the flue gas. Fig. 4 presents the variation of the water vapor concentration along the channel. Considering the concentration in the centerline, the length of the channel required to maximize the condensation of vapor is around 0.005, 0.01, 0.05, and 0.1 m for the inlet velocity of 0.5, 1, 5, and 10 m/s, respectively.

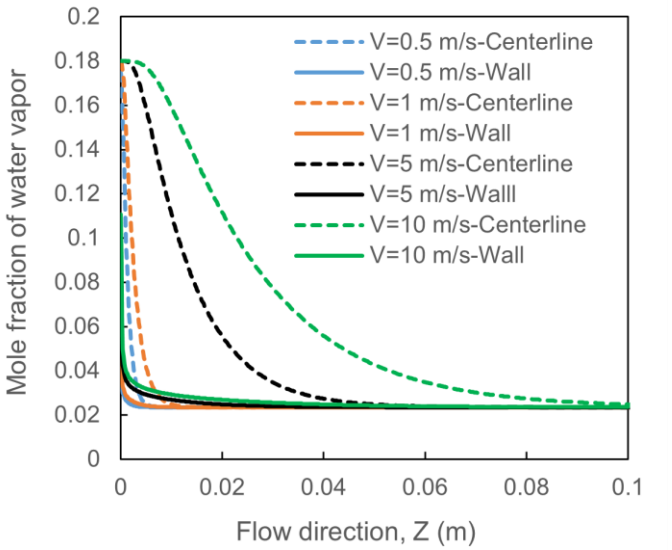

Figure 4 Variation of mole fraction of vapor along the channel, in the centerline and on one of the walls, for different velocity inlets.

A similar behavior can be observed for the temperature profile along the channel as shown in Fig. 5. This also indicates the length required for sensible heat transfer, which is slightly longer than that for latent heat recovery.

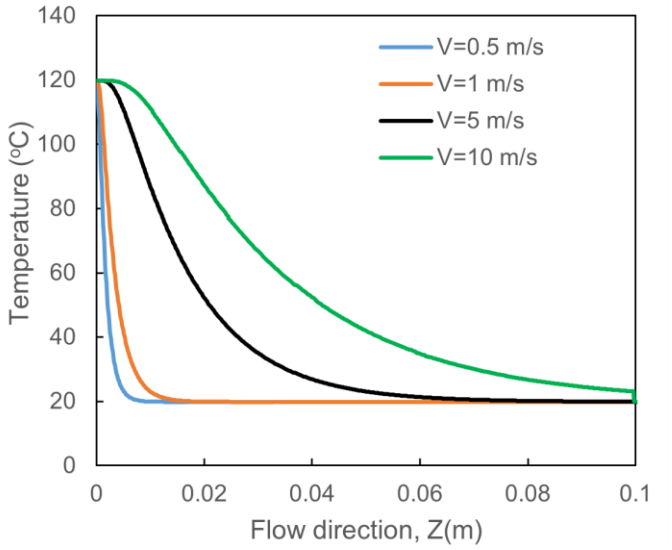

Figure 5 Variation of the mixture's temperature along the channel centerline for different velocity inlets.

As declared so far, the total amount of heat transferred through the liquid film on the wall consist of sensible heat, mainly caused by convective heat transfer, and latent heat, caused by condensation of vapor. Fig. 6 illustrates the summation of these two parts along one wall of the channel; the total heat flux in each cross section is four times the value shown in Fig. 6. As the water vapor content and bulk flow temperature decrease along the flow the local total heat flux decreases continuously.

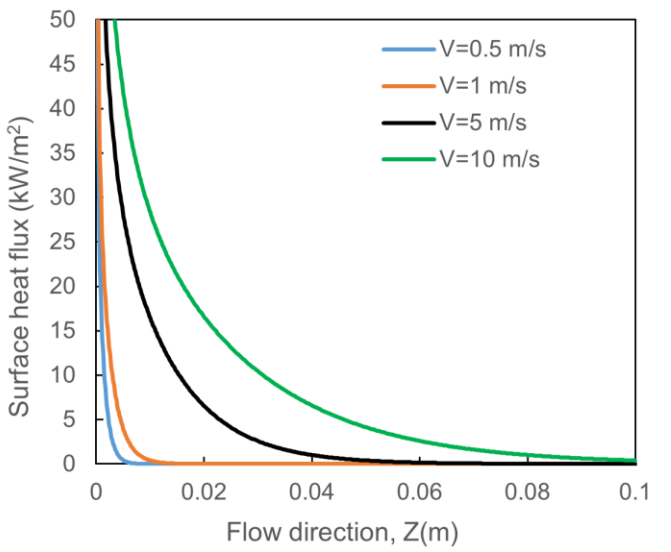

Figure 6 Variation of local heat flux along the channel wall for different velocity inlets.

The present condensation model is capable of predicting the liquid film characteristics, including film thickness. Fig. 7, depicts the liquid film formation on the middle of the wall. This parameter is crucial to ensuring that the mini-channel does not become clogged due to liquid formation. The film thickness reaches its maximum value quickly at low flue gas flow rates, but as flow rates increase film grows slower. Due to the higher shear stress in the main flow, the film becomes thinner as mixture flow rate increases.

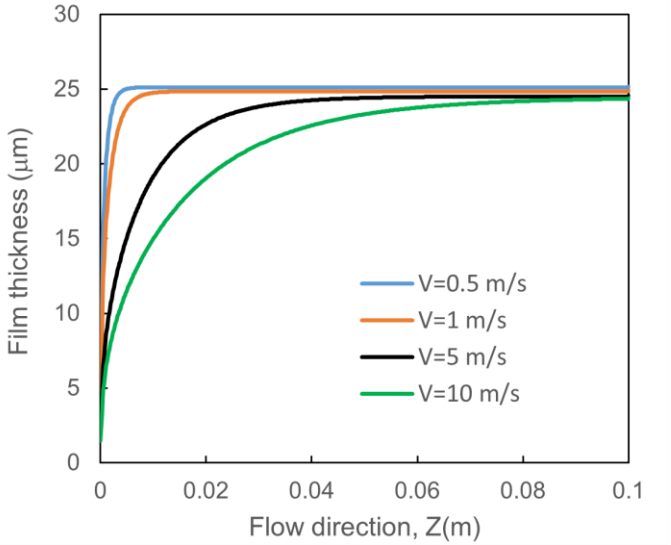

Figure 7 Variation of liquid film along the channel wall for different mixture velocity inlets.

ACKNOWLEDGMENT

The authors acknowledge the Syilx Okanagan Nation for the use of their unceded territory, the land on which the research was conducted. The authors wish to acknowledge the financial support provided by Mitacs and FEED Engineering Inc. through the Mitacs Accelerate program. We would like also to thank the CMC microelectronics for their support on ANSYS software licenses.

REFERENCES

[1] V. Dharma Rao, V. Murali Krishna, K. v. Sharma, and P. V. J. M. Rao, "Convective condensation of vapor in the presence of a non-condensable gas of high concentration in laminar flow in a vertical pipe," International Journal of Heat and Mass Transfer, vol. 51, no. 25–26, 2008, doi: 10.1016/j.ijheatmasstransfer.2008.03.027.

[2] T. H. Phan, S. S. Won, and W. G. Park, "Numerical simulation of air–steam mixture condensation flows in a vertical tube," International Journal of Heat and Mass Transfer, vol. 127, 2018, doi: 10.1016/j.ijheatmasstransfer.2018.08.043.

[3] G. Zschaeck, T. Frank, and A. D. Burns, "CFD modelling and validation of wall condensation in the presence of non-condensable gases," Nuclear Engineering and Design, vol. 279, 2014, doi: 10.1016/j.nucengdes.2014.03.007.

[4] M. Punetha and S. Khandekar, "A CFD based modelling approach for predicting steam condensation in the presence of non-condensable gases," Nuclear Engineering and Design, vol. 324, 2017, doi: 10.1016/j.nucengdes.2017.09.007.

[5] G. Vijaya Kumar et al., "Implementation of a CFD model for wall condensation in the presence of non-condensable gas mixtures," Applied Thermal Engineering, vol. 187, 2021, doi: 10.1016/j.applthermaleng.2021.116546.

[6] J. de Li, "CFD simulation of water vapour condensation in the presence of non-condensable gas in vertical cylindrical condensers," International Journal of Heat and Mass Transfer, vol. 57, no. 2, 2013, doi: 10.1016/j.ijheatmasstransfer.2012.10.051.

[7] L. Liu, W. Chen, C. Wang, and C. Hu, "CFD analysis of steam condensation with air in the tubes bundle channel under natural convection conditions," Annals of Nuclear Energy, vol. 162, 2021, doi: 10.1016/j.anucene.2021.108510.

[8] "ANSYS Fluent Theory Guide, 2021 R2, Section 7.1.1.1. Species Transport Equations."

[9] W. Ambrosini, M. Bucci, N. Forgione, A. Manfredini, and F. Oriolo, "Experiments and modelling techniques for heat and mass transfer in light water reactors," Science and Technology of Nuclear Installations, vol. 2009. 2009. doi: 10.1155/2009/738480.

[10] V. Ferrara, "Computational analysis of condensation in the presence of noncondesable gases in the CONONfacility.," thesis, 2012.

[11] W. Ambrosini et al., "Lesson learned from the SARNET wall condensation benchmarks," Annals of Nuclear Energy, vol. 74, no. C, 2014, doi: 10.1016/j.anucene.2014.07.014.